Astronomy & Astrophysics manuscript no. v5.1 September 18, 2014
(DOI: will be inserted by hand later)

Tests of General relativity with planetary orbits and Monte Carlo simulations

A. Fienga[1,2], J. Laskar[2], P. Exertier[1], H. Manche[2], M. Gastineau[2]

[1] Géoazur, CNRS/UMR7329, Observatoire de la Côte d'Azur, Valbonne, France
[2] IMCCE, CNRS/UMR8028, Observatoire de Paris, Paris, France

September 18, 2014

Abstract. Based on the new developped planetary ephemerides INPOP13c, determinations of acceptable intervals of General Relativity violation in considering simultaneously the PPN parameters β, PPN γ, the flattening of the sun $J_2^\odot$ and time variation of the gravitational mass of the sun μ are obtained in using Monte Carlo simulation coupled with basic genetic algorithm. Possible time variations of the gravitational constant G are also deduced. Discussions are lead about the better choice of indicators for the goodness-of-fit for each run and limits consistent with general relativity are obtained simultaneously.

Key words. Celestial mechanics – ephemerides – gravitation – methods: numerical, data analysis

arXiv:1409.4932v1 [astro-ph.EP] 17 Sep 2014

1. Introduction

Since the first publications of the theory of General Relativity (Einstein (1913)), the dynamics of the solar system has demonstrated its efficiency for testing gravity theories. Examples can be given such as the measurements of the advance of perihelia (Le Verrier (1859)) of Mercury's orbit, firstly observed and then explained by General Relativity (GR), or of the asteroid Icarus's orbit (Francis (1965)), or the measurement of the deflexion of light by the Sun during the cruise phase of Cassini probe (Bertotti et al. (2003)). Direct implementations of alternative metrics in the equations of motion of the planets of the solar system and of spacecraft orbiting planets were also introduced (Müller et al. (2008), Konopliv et al. (2011), Hees et al. (2012)) stressing the interest of using the solar system as a laboratory for testing alternative modelings of gravity. Tests based on the analysis of MESSENGER spacecraft tracking data used in the construction of INPOP ephemerides or the Cassini tracking data for the JPL DE ephemerides have also demonstrated the impact of using planetary ephemerides for eliminating possible values of parameters characterizing alternative theories of gravity (Fienga et al. (2010), Verma et al. (2014), Hees et al. (2014)).

Planetary ephemerides can thus be used as a very efficient tool for several scientific applications. For example, with the INPOP planetary ephemerides developed since 2003, determinations of the flattening of the Sun $J_2^\odot$, of the PPN parameters β and γ, and estimates of the perihelion advances of the 8 planets of the solar system have been obtained with considerable precision. No new advance and no β and γ deviations from unity could be exhibited, confirming the validity of general relativity to the level of 10^{-5} (Fienga et al. (2011),Verma et al. (2014)). INPOP constraints on supplementary advances of nodes and perihelia of the planets give stringent constraints on cosmological models of gravity such as MOND (Blanchet & Novak (2011)). The INPOP limits of violation for PPN β and γ are important constraints for certain type of tensor-scalar theories where cosmological evolution exhibits an attractor mechanism towards GRT (Damour & Nordtvedt (1993)) or in string-inspired scalar-tensor theories where the scalar field can decouple from matter (Damour & Polyakov (1994)).

Finally, some phenomenological tests are related to the constancy of the Newtonian gravitational constant G in time. Variations of G are produced e.g. by alternative theories of gravity like tensor-scalar theory (see e.g. Damour et al. (1990) and Uzan (2003)) or by some models of Dark Energy (Steinhardt & Wesley (2009); Füzfa & Alimi (2007)). The $\dot{G}/G$ ratio is now constrained at the level of 10^{-13} with LLR analysis (Williams et al. (2004)) but no tests combining simultaneously modifications of PPN formalism, variation of the sun flattening and of the Newtonian gravitational constant were done. Some estimations of PPN violations and of $\dot{G}$ were obtained by Pitjeva & Pitjev (2013).

The purpose of this work is to make the first simultaneous determinations of possible variations from unity of PPN parameters β, γ and of non-zero value for $\dot{G}$ but also in including the determination of the flattening of the Sun. We consider the equation of the advance in perihelia $\Delta\dot{\varpi}$ for any planet of the solar system in the PPN formalism as a good tool for monitoring the question of the determination of these parameters. We have:

$$\Delta\dot{\varpi} = \frac{2\pi(2\gamma-\beta+2)GM_\odot(t)}{a(1-e^2)c^2} + \frac{3\pi J_2^\odot R_\odot^2}{a^2(1-e^2)c^2} + \Delta\dot{\varpi}_{AST} \qquad (1)$$

where a and e are the semi-major axis and the eccentricity of the planet orbit respectively, $R_\odot^2$ is the Sun radius respectively

and $\Delta\dot{\varpi}_{AST}$ is the advance of the planet perihelia induced by the perturbations of the asteroids. The PPN term is directly related to the Sun flatness $J_2^\odot$ but also to any variation of G through $GM_\odot(t)$. The term induced by the asteroid perturbations will be taken care by the iterative fit of the ephemerides to the observations and by the determination of the masses of the perturbing asteroids. The disentangling of the PPN terms with Sun $J_2^\odot$ will be reinforced by the use of the eight orbits of the solar system planets and the introduction of eight different values for the semi-major axis a. A non-unity PPN γ is also introduced in the equation of the deflexion of light required for the computation of residuals as well as in the analysis of spacecraft tracking data. However as it was demonstrated in Verma (2013), the orbital variations induced by the change in the values of the PPN γ and β parameters can be absorbed during the fit and the construction of the spacecraft orbit. No iteration is then required and only the impact of the modified deflexion of light on the deduced planetary light time has to be taken into account.

By considering simultaneously the construction of planetary ephemerides built with values of PPN parameters different from unity, with a gravitational constant G varying with time and a non-zero Sun flattening, we obtain the first consistent tests of this type based on planetary ephemerides. However, because of the important number of simulations required by this approach, we use optimization method and more specifically genetic algorithm. Since their first implementations in astrophysics by Charbonneau (1995), the genetic algorithms and the evolutionary computation have been intensively used in the dynamical studies of the extra-solar systems (Nowak et al. (2013), Migaszewski et al. (2012), Horner et al. (2012), Goździewski et al. (2012)) but also in other fields such as astrosismology, binary physics, planetology (Karnath et al. (2013), Siqueira Mello et al. (2014), Henke et al. (2013)). For the extra-solar planetary systems, the goal is to determine which combinations of planets can generate a radial velocity signature very similar to the one observed. Due to the constraints imposed by the dynamics, the algorithms applied for this type of studies can be very complex (Beaugé et al. (2012)). In our case, only starting intervals for the varying parameters (PPN β, γ, $J_2^\odot$ and $\dot{\mu}/\mu$) are given and a simple two crossovers algorithm is used. The applied genetic algorithm is fully described in section 4.1 and several fitness functions are discussed in sections 4.1 and 5. Corresponding results are presented in sections 4.2 and 5.3.

2. Implementation of GR tests in INPOP13c

The computations performed in this work are based on the new version of the INPOP ephemerides, INPOP13c. The following section introduces INPOP13c and the necessary modifications of the equations of motion in order to introduce the time variations of the Newtonian gravitational constant.

2.1. Description of INPOP13c

By the use of the tracking data of the MESSENGER mission, INPOP13a becomes an important tool for testing General Relativity close to the Sun (Verma et al. (2014)). The MESSENGER mission was indeed the first mission dedicated to the study of Mercury. The spacecraft orbits the smallest and closest to the sun planet of the solar system since 2011. In (Verma et al. (2014)) are described the methods and procedures used for the analysis of the MESSENGER Doppler and range data included in the construction of the Mercury improved ephemerides, INPOP13a as well as the determination of acceptable intervals of non-unity values for the PPN β and γ.

INPOP13c is an upgraded version of INPOP13a, fitted to LLR observations, and including new observables of Mars and Venus deduced from MEX, Mars Odyssey and VEX tracking (Morley (2012), Morley (2013) , Marty (2013)). Table A.1 of appendix A resumes the data samples and the obtained residuals with INPOP13c and INPOP10e common to the two ephemerides when Table A.2 exhibits the residuals obtained for the data samples added since INPOP10e. Thanks to this supplementary material, INPOP13c faces a better extrapolation capability of the Mars ephemerides as well as better consistencies between DE and INPOP ephemerides. For more details, tables and plots can be found in Fienga et al. (2014).

The INPOP13c adjustment of the gravitational mass of the sun was performed as recommended by the IAU resolution B2 as well as the sun oblateness ($J_2^\odot$), the ratio between the mass of the earth and the mass of the moon (EMRAT) and the mass of the Earth-Moon barycenter. Estimated values are presented on Table 1.

2.2. Implementation of GR tests

2.2.1. PPN β, γ and $J_2^\odot$

Based on the procedures described in Fienga et al. (2010), Fienga et al. (2011) and Verma et al. (2014), evaluations of acceptable values of PPN β and γ were obtained for previous versions of INPOP by comparisons of the postfit residuals obtained with planetary ephemerides numerically integrated and fitted with values of β and γ different from unity. Such procedure was set up to answer to questions rose by alternative theories of gravitation proposing solar systems facing non-zero PPN parameters. As described in Fienga et al. (2011) and Verma et al. (2014), a grid of sensitivity of PPN β and γ but also of supplementary advances in the perihelia and the nodes of the planets was set up and compared to observations. Such a grid is built by constructing ephemerides with non-unity PPN parameters, numerically integrated and fitted to the same data sample as the regular INPOP. We then consider the maximum differences between the postfit residuals obtained with the ephemerides built in a non relativistic frame and INPOP. The limit chosen for defining the acceptable intervals of PPN parameters leading to postfit residuals close to INPOP was largely discussed in Verma et al. (2014) leading to an optimized value of 25%.

2.2.2. Variation of the gravitational constant

For this work, we added in the INPOP dynamical model the possibility of constraining variations of the gravitational mass of the sun, μ, considering a variation of the mass of the sun noted $\dot{M}_\odot$ (often interpreted in stellar physics as the Sun mass

Table 1: Values of parameters obtained in the fit of INPOP13c, INPOP10e and DE430 (Folkner et al. (2014)) to observations.

	INPOP13c $\pm 1\sigma$	INPOP10e $\pm 1\sigma$	DE430 $\pm 1\sigma$
(EMRAT-81.3000)$\times 10^{-4}$	(5.694 ± 0.010)	(5.700 ± 0.020)	(±)
$J_2^\odot \times 10^{-7}$	(2.30 ± 0.25)	(1.80 ± 0.25)	1.80
$GM_\odot$ - 132712440000 [$km^3.s^{-2}$]	(44.487 ± 0.17)	(50.16 ± 1.3)	40.944
AU - 1.49597870700 $\times 10^{11}$ [m]	0.0	0.0	(-0.3738 ± 3)
$[M_\odot / M_{EMB}]$ - 328900	0.55314 ± 0.00033	0.55223 ± 0.004	0.55915 ± NC

loss) and a variation of the gravitational constant $\dot{G}$. We have with $\mu = G \times M_\odot$:

$$\frac{\dot{\mu}}{\mu} = \frac{\dot{G}}{G} + \frac{\dot{M}_\odot}{M_\odot} \quad (2)$$

At each step t of the numerical integration of the INPOP equations of motion, we then estimate :

$$M_\odot(t) = M_\odot(J2000) + (t - J2000) \times \dot{M}_\odot \quad (3)$$
$$G(t) = G(J2000) + (t - J2000) \times \dot{G} \quad (4)$$
$$\mu(t) = G(t) \times M_\odot(t) \quad (5)$$

$\dot{\mu}/\mu$ plays also a role in the computation of the Shapiro delay of the observables (see Moyer (2000)). In this case, the value of μ corresponding to the date of the observation is computed with Equation 5 and re-introduced in the Shapiro delay equation (8-38) given in Moyer (2000).

Tests are then operated by considering different values of $\dot{\mu}/\mu$. We use for $M_\odot(J2000)$ the fitted mass of the sun as estimated for each planetary ephemerides (the value obtained for INPOP13c is given in Table 1) and for $G(J2000)$ the Newtonian gravitation constant as defined by the IAU (Luzum et al. (2011)). We then deduce values of $\dot{G}/G$ in considering a fixed value for the Sun total mass loss (including radiation and solar winds):

$$\frac{\dot{M}_\odot}{M_\odot} = (-0.55 \pm 0.15) \times 10^{-13}\ \mathrm{yr}^{-1}$$

extracted from solar physics measurements and variations of $\dot{M}_\odot/M_\odot$ during the 11-year solar cycle (Pinto et al. (2011)).

3. Monte Carlo simulations

3.1. Principle

Following the strategy described above, an uniform sampling of PPN β, γ, $J_2^\odot$ and $\dot{\mu}/\mu$ was built in order to be used for the construction of planetary ephemerides adjusted to observations. Postfit residuals were obtained after several iterations and compared to those obtained with the nominal planetary ephemerides INPOP13c built in the GR framework with $\beta = \gamma = 1$, $\dot{\mu}/\mu = 0$ and $J_2^\odot = 2.3$ as given in Table 1. The plots of the left-hand side of Figure 1 show the uniform distribution of the GR parameters obtained after 4000 runs. The right-hand side plots give the histograms of one possible selection of (β, γ, $J_2^\odot$, $\dot{\mu}/\mu$) (see section 3.2). The intervals of the uniform distributions were chosen larger than the present limits found in the literature and gathered in Table 2. For the PPN parameters β and γ, we selected an interval of $\pm 15 \times 10^{-5}$ enclosing VLBI and LLR determinations (Williams et al. (2009), Lambert & Le Poncin-Lafitte (2009)). For the Sun flattening, our interval from 1.6×10^{-7} to 2.8×10^{-7} also includes the values found in the literature mainly extracted from planetary ephemerides construction (Verma et al. (2014), Fienga et al. (2009)).

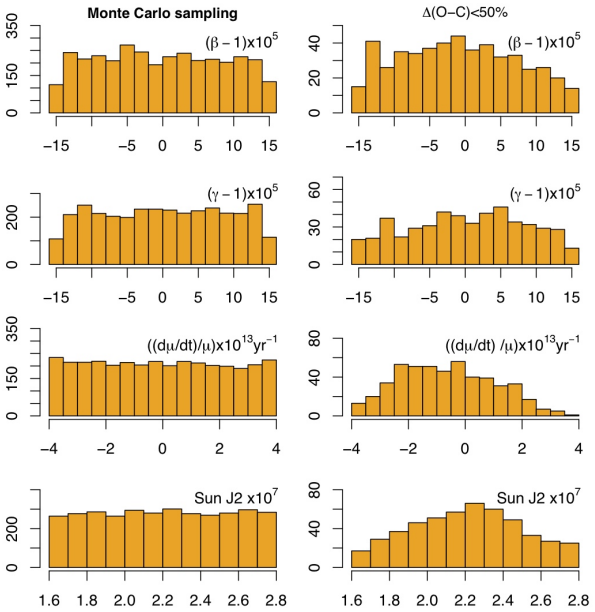

Fig. 1: On the left: histograms of the uniform random values for PPN β, PPN γ, $J_2^\odot$, and $\dot{\mu}/\mu$ parameters used for the construction of the planetary ephemerides for the Monte Carlo simulation. On the right: histograms of the distribution of the PPN β, PPN γ, $J_2^\odot$, and $\dot{\mu}/\mu$ parameters corresponding to the selected ephemerides using the criteria of 50% differences of postfit residuals. See section 3.2

3.2. First Results

After the constructions of the planetary ephemerides based on an uniform sampling of values for (β, γ, $J_2^\odot$, $\dot{\mu}/\mu$), postfit residuals were obtained and compared with those given by INPOP13c. Criteria are then chosen for selecting values of (β, γ, $J_2^\odot$, $\dot{\mu}/\mu$) leading to ephemerides close to INPOP13c. For these selected values, it is not possible to say in the light of the present accuracy of the observations if they induced noticeable violation of planetary dynamics. A possible approach for the

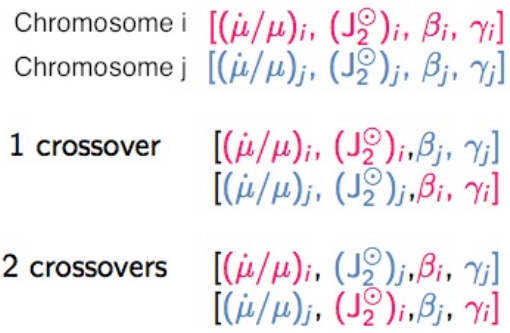
Chromosome i $[(\dot\mu/\mu)_i, (J_2^\odot)_i, \beta_i, \gamma_i]$
Chromosome j $[(\dot\mu/\mu)_j, (J_2^\odot)_j, \beta_j, \gamma_j]$
1 crossover
$[(\dot\mu/\mu)_i, (J_2^\odot)_i, \beta_j, \gamma_j]$
$[(\dot\mu/\mu)_j, (J_2^\odot)_j, \beta_i, \gamma_i]$
2 crossovers
$[(\dot\mu/\mu)_i, (J_2^\odot)_j, \beta_i, \gamma_j]$
$[(\dot\mu/\mu)_j, (J_2^\odot)_i, \beta_j, \gamma_i]$

Fig. 2: Scheme of the genetic algorithm procedure.

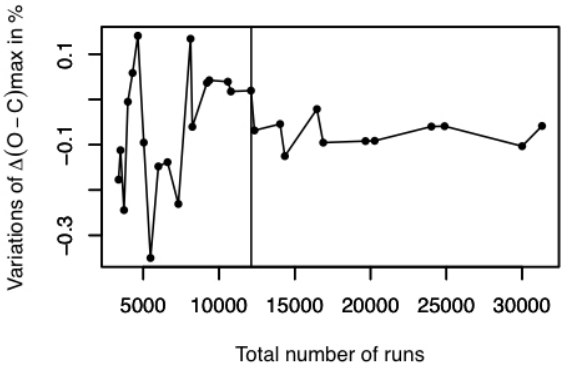

Fig. 3: Convergence of the Genetic Algorithm. The x-axis is the total number of runs accumulated over the generations while on the y-axis are plotted the differences for the average maximum differences $\Delta(O-C)_{max}$ in post residuals obtained for each generation. The dashed line indicates the 18th generation reaching a total number of 12125 runs.

selection of such ephemerides and (β, γ, $J_2^\odot$, $\dot\mu/\mu$) sampling is to consider the maximum differences noted $\Delta(O-C)_{max}$ between the postfit residuals of the non-GR ephemerides and those of INPOP13c. This strategy was used previously in Fienga et al. (2011) and Verma et al. (2014) and lead to a threshold of 25% for $\Delta(O-C)_{max}$ as an appropriate limit for considering noticeable violations of planetary dynamics.

Because of the increase of the number of free parameters in the present simulations compared to the previous publications where only PPN β and γ were randomly modified, the postfit difference threshold was rose up to 50% in a first attempt to define violation limits. Only 15% of the 4000 runs give postfit residual differences to INPOP13c below 50% and only 1.4% runs give differences below 25% . On the right-hand side on Figure 1, the distributions of values for β, γ, $J_2^\odot$ and $\dot\mu/\mu$ parameters corresponding to 15 % of the selected ephemerides are plotted. As it appears, except perhaps for $J_2^\odot$, the selected values do not show a gaussian distribution even after postfit residual selections. Because on these results, an optimization of the Monte Carlo simulations based on a genetic algorithm was set up.

4. Optimized MC simulations with Genetic Algorithm

4.1. Principle

We consider a genetic algorithm with two crossovers[1] and a probability of mutation of 10 % as illustrated on Figure 2. The considered chromosome[2] is here one set of four values of (β, γ, $J_2^\odot$, $\dot\mu/\mu$) and the individual is an INPOP planetary ephemerides built in using the values of (β, γ, $J_2^\odot$, $\dot\mu/\mu$), numerically integrated and fitted to observations in an iterative process. The fitness of each individual is the difference of its postfit residuals to INPOP13c noted $\Delta(O-C)$.

A total of 35800 runs spread over 30 generations were computed on the Paris Science et Lettres mesocentre with NEC 1472 kernels on 92 nodes. Two nodes were allocated for this work allowing 12 runs over 1 hour, one run representing the construction of about four numerically integrated and iteratively fitted planetary ephemerides. The 4000 runs of the Monte Carlo simulation presented in section 3.1 were used to initialize the algorithm as the generation 0.

We stop the generational process until the average change in the maximum differences of postfit residuals $\Delta(O-C)_{max}$ is stabilized. As one can see on Figure 3, these differences stabilized at about 12 000 runs corresponding to the 18th generation. A clear change of regime is then obtained with a dispersion of 0.14% before the generation 18 and of 0.03% after.

4.2. Results

On Figure 4 are given the percentages of runs with $\Delta(O-C)_{max} < 50\%$ and $\Delta(O-C)_{max} < 25\%$. The rates of selected ephemerides increase with the number of runs reaching 50 % of the total runs for $\Delta(O-C)_{max} < 50\%$ and 14 % for $\Delta(O-C)_{max} < 25\%$. The Gaussianity of the (β, γ, $J_2^\odot$, $\dot\mu/\mu$) samples corresponding to the selected ephemerides is also improved as one can see on the cumulative histograms of Figure 5 and on the histograms of Figure 6. It is then possible to estimate mean values and $1-\sigma$ standard deviations of the sample of PPN β, γ, $J_2^\odot$ and $\dot\mu/\mu$ corresponding to the selected ephemerides. As one can see on Figure 7, the dispersion of the selected samples of (β, γ, $J_2^\odot$, $\dot\mu/\mu$) decreases with the number of solutions and the percentages of selected ephemerides. The reduction of the dispersion value is generally of about a factor 2 from the generation 0 to the final generation.

The mean and σ obtained from the description of the distribution of the (PPN β, PPN γ, $J_2^\odot$, $\dot\mu/\mu$) samples corresponding to the selected ephemerides give the intervals of acceptable violation of general relativity on the basis of postfit residual differences to INPOP13c. Table 2 gathers these estimations labelled MC+ GA 50% for the samples of parameters inducing $\Delta(O-C)_{max} < 50\%$ and MC+ GA 25% for samples inducing $\Delta(O-C)_{max} < 25\%$, together with values found in the literature. The obtained intervals are very competitive even if the inter-

[1] Genetic operator used for varying the parameters from one generation to another. In our case, a simple swap is used.Magnin (1998)

[2] set of parameters defining a proposed solution to the problem and randomly modified by the algorithm. Magnin (1998)

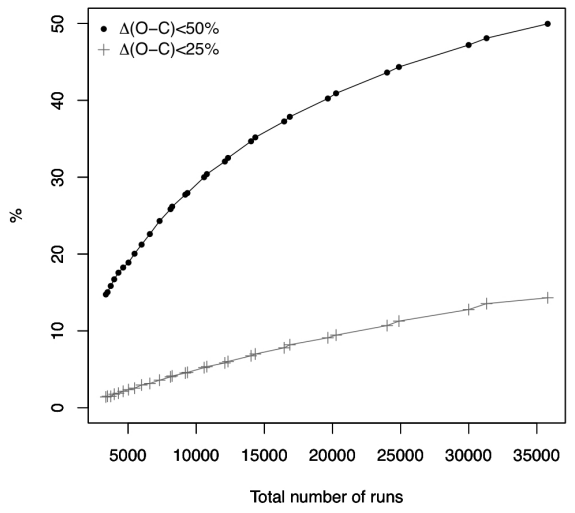

Fig. 4: Evolution of the number of selected ephemerides using the criteria of 50% and of 25% for $\Delta(O-C)_{max}$ respectively.

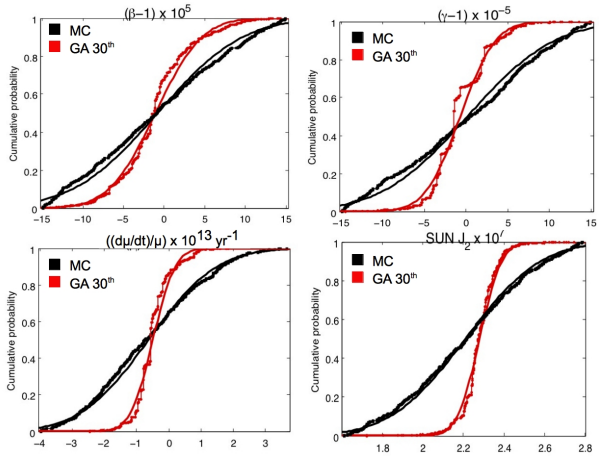

Fig. 5: Cumulative histograms of (PPN β, PPN γ, $J_2^\odot$, $\dot{\mu}/\mu$) for the generation 0 of ephemerides selected with the $\Delta(O-C)_{max} < 50\%$ (noted MC and colored in black) and for the 30th generation (notes GA 30^{th} in red) also selected with $\Delta(O-C)_{max} < 50\%$. The full lines correspond to the cumulative histograms of the normal distributions fitted on the distributions of the first generation and the 30th generation.

vals for β and γ are larger than those obtained with INPOP13a. This was expected as variations of $J_2^\odot$ and $\dot{\mu}/\mu$ were included in these results but not in INPOP13a. However other criteria can be used for selecting the ephemerides and for defining new thresholds.

5. The resampling criteria

5.1. Definition

The differences between two least squares adjustments can be characterized by the χ^2 values obtained for each fit. The χ^2 is

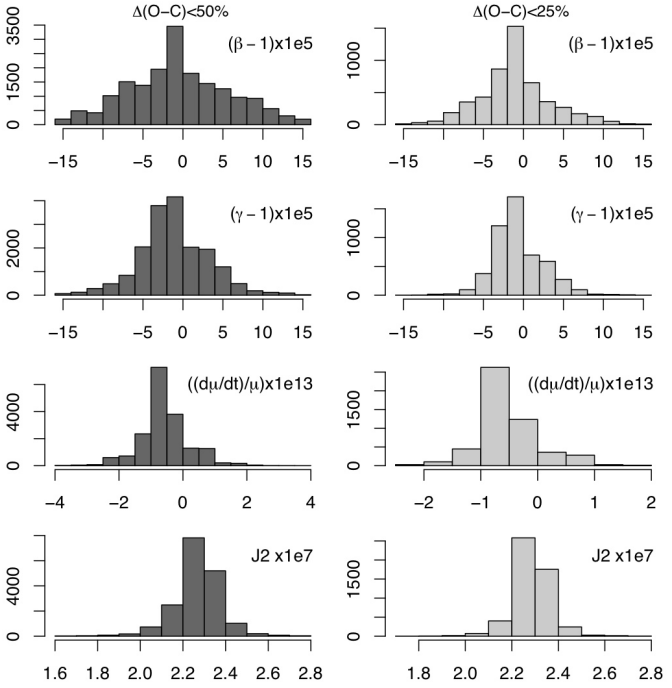

Fig. 6: Histograms of the distribution of the PPN β, PPN γ, $J_2^\odot$, and $\dot{\mu}/\mu$ parameters corresponding to the selected ephemerides using the criteria of 50% and the 25% differences of postfit residuals respectively, after 30 generations.

usually given by

$$(\mathrm{N}-\mathrm{M})\,\chi^2 = \sum_{i=1}^{N} \frac{(O-C)_i^2}{\sigma_i^2}$$

where N is the number of data used for the adjustment, M the number of fitted parameters, σ_i the estimated variance of the observation i and $(O-C)_i$ is the postfit residual of the data i. In the theory of least squares, the minimization of χ^2 is the main criteria for the convergency of the adjustment. Considering the difference between two ephemerides by their χ^2 differences, one characterizes how well the two dynamical modelings represent the weighted observations. We have then compared the χ^2 obtained with a random (PPN β, PPN γ, $J_2^\odot$, $\dot{\mu}/\mu$) ephemerides with the χ^2 of INPOP13c. We note $\delta\chi^2$ such difference with:

$$\delta\chi^2 = \chi^2_{(\beta,\gamma,J_2^\odot,\dot{G}/G)} - \chi^2_{\mathrm{IN}}$$

The histogram of the obtained differences noted $\delta\chi^2$ is plotted on Figure 8. As one can see, the differences can reach several orders of magnitude but can also be very small. In order to make a selection of which differences are negligible compared to the INPOP13c uncertainties, we use a method based on the resampling of the observational data sets as the observational uncertainties are the main source of error for the planetary ephemerides (section 5.2).

5.2. Resampling method

One way to evaluate the planetary ephemeris uncertainties in terms of χ^2 is to consider the differences of the χ^2 induced by

Table 2: Results compared to values found in the literature.

Method	Selected runs	PPN $\beta - 1$ $\times 10^{-5}$	PPN $\gamma - 1$ $\times 10^{-5}$	$\dot{\mu}/\mu$ $\times 10^{13}$ yr^{-1}	$\dot{G}$/G $\times 10^{13}$ yr^{-1}	$J_2^\odot$ $\times 10^7$
This paper						
MC	3694	-0.8 ± 8.2	0.2 ± 8.2	-0.63 ± 1.66	0.04 ± -0.08	1.81 ± 0.29
MC + GA 50 %	17888	-0.49 ± 6.31	-1.19 ± 4.43	-0.56 ± 0.76	-0.01 ± 0.91	2.26 ± 0.11
MC + GA 25 %	5120	-1.06 ± 4.46	-0.75 ± 3.23	-0.51 ± 0.54	0.04 ± 0.69	2.28 ± 0.08
MC + GA H_{RS}	8537	-0.01 ± 7.10	-1.67 ± 5.25	-0.37 ± 0.76	0.18 ± 0.91	2.22 ± 0.14
< MC + GA (50 % + RS) >		-0.25 ± 6.70	-1.48 ± 4.82	-0.46± 0.76	0.09 ± 0.91	2.24± 0.125
Planetary ephemerides						
DE (Konopliv et al. (2011))		4 ± 24	fixed to (2.1 ± 2.3)	0.0	0.0	fixed to 1.8
		fixed	18 ± 26	0.0	0.0	fixed to 1.8
		0.0	0.0	0.1 ± 1.6	0.65 ± 1.75*	fixed to 1.8
DE (Folkner et al. (2014))		0.0	0.0	0.0	0.0	2.1 ± 0.70
EMP (Pitjeva & Pitjev (2013))		-2 ± 3	4 ± 6			2.0 ± 0.2
				-0.63 ± 0.43	-0.08 ± 0.58*	
INPOP13a (Verma et al. (2014))		0.2 ± 2.5	-0.3 ± 2.5	0.0	0.0	2.40 ± 0.20
INPOP10a (Fienga et al. (2011))		-4.1 ± 7.8	-6.2 ± 8.1	0.0	0.0	2.40 ± 0.25
INPOP08 (Fienga et al. (2009))		7.5 ± 12.5	0.0	0.0	0.0	1.82 ± 0.47
LLR						
Williams et al. (2009)		12 ± 11	fixed to (2.1 ± 2.3)		0.0	
Williams & Folkner (2009)		0.0	0.0		± 3	
Hofmann et al. (2010)		0.0	0.0		-0.7 ± 3.8	
		3 ± 13	fixed to (2.1 ± 2.3)		0.0	
Other technics						
Cassini (Bertotti et al. (2003))		0.0	2.1 ± 2.3	0.0	0.0	NC
VLBI (Lambert & Le Poncin-Lafitte (2009))		0.0	-8 ± 12	0.0	0.0	fixed
Planck + Brans-Dicke (Li et al. (2013))					-1.315± 2.375	
Binary pulsar (Kaspi et al. (1994))					40± 50	
Heliosismology (Guenther et al. (1998))					0± 16	
Big Bang nucleosynthesis (Bambi et al. (2005))					0 ± 4	

* *This value is not the published one but is calculated in using the value of $\dot{M}/M$ given in section 2.2.2*

the variances and bias of the observational data sets used for the fit. An interesting tool is then to use a resampling technique. By removing randomly a part of the observational sample used for the fit (Busing et al. (1999)), one can estimate the robustness of the estimated parameters but also a realistic estimation of the postfit residuals and of the χ^2(Cook & Weisberg (1982), Fay (1985)). The variations of the χ^2 will indicate the sensibility of the fit to the observational sampling. We operate 101 runs by removing randomly 10% of the INPOP data sample. We then estimate the variation of the χ^2 in comparison to the χ^2 obtained for INPOP13c. We note:

$$\Delta\chi^2_j = \chi^2_j - \chi^2_{\rm IN}$$

with $j = 1, ...101$. Such $\Delta\chi^2$ gives an estimation of the variation of the χ^2 induced by the variance and bias in the data sampling. We keep as a threshold the maximum value of $\Delta\chi^2$ obtained after 101 tests of random modification of the data sample and labelled $\Delta\chi^2_{max}$. It gives the limit for the $\delta\chi^2$ differences: a planetary ephemerides built with a random selection of (PPN β, PPN γ, $J_2^\odot$, $\dot{\mu}/\mu$) is close to INPOP13c if the obtained χ^2 does not differ from the INPOP13c χ^2 by more than the maximum χ^2 differences induced by the data sample bias and variances. In the following, this test will be called the resampling criteria or noted H_{RS}.

5.3. Results

On figure 10, are plotted the number of selected random (PPN β, PPN γ, $J_2^\odot$, $\dot{\mu}/\mu$) ephemerides based on the resampling criteria. As one can see, the number of selected ephemerides increases with the number of runs. The convergence of the algorithm is illustrated on Figure 11 where the average values of the $\delta\chi^2$ for each generation are plotted regarding the cumulated number of runs. The stabilization is obtained before the 35800 runs (30th generation).

As one can see on figure 12, the Gaussianity of the (PPN β, PPN γ, $J_2^\odot$, $\dot{\mu}/\mu$) parameters corresponding to the selected ephemerides improves with the runs. Furthermore, on figure 13, it also appears that the uncertainties deduced from these gaussian distributions of (PPN β, PPN γ, $J_2^\odot$, $\dot{\mu}/\mu$) also decrease with the number of runs. For illustration we give on figure 14 the histograms of the (PPN β, PPN γ, $J_2^\odot$, $\dot{\mu}/\mu$) parameters deduced for the full analysis of the 35800 runs (30^{th} generation). The mean values and 1-σ standard deviations of (PPN β, PPN γ, $J_2^\odot$, $\dot{\mu}/\mu$) parameters extracted from these histograms are given on Table 2.

In general, in comparison to the previous criteria of ephemeris selection based on the maximum differences in the postfit residuals (see section 3.2), the criteria based on the estimation of the variations of the χ^2 are more selective. But in

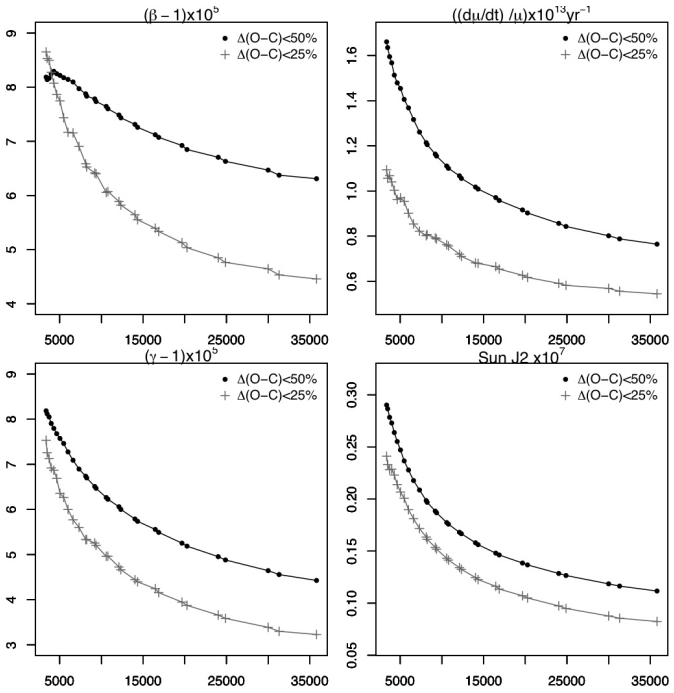

Fig. 7: Evolution with the total number runs of the 1-σ of the gaussian distribution of the PPN β, PPN γ, $J_2^{\odot}$, and $\dot{\mu}/\mu$ parameters corresponding to the selected ephemerides using $\Delta(O-C)_{max} < 50\%$ and $\Delta(O-C)_{max} < 25\%$ respectively.

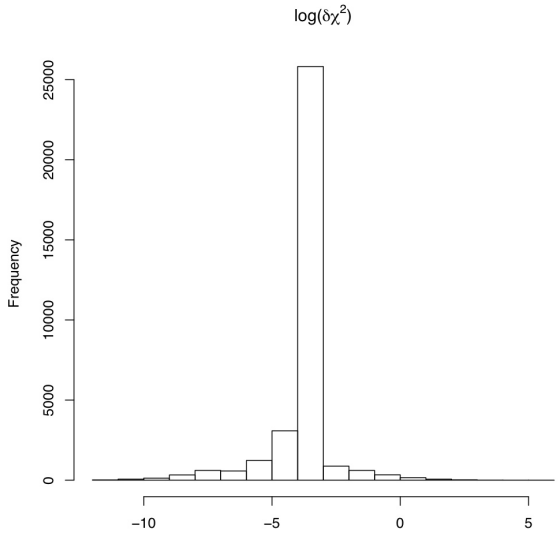

Fig. 8: Histogram of the log of the differences $\delta\chi^2$ between the χ^2 obtained for INPOP13c and the χ^2 computed during the construction of the random (PPN β, PPN γ, $J_2^{\odot}$, $\dot{\mu}/\mu$) ephemerides.

the same time, the gaussian distributions of the (PPN β, PPN γ, $J_2^{\odot}$, $\dot{\mu}/\mu$) parameters are slightly larger leading to less restrictive intervals of possible violation of general relativity.

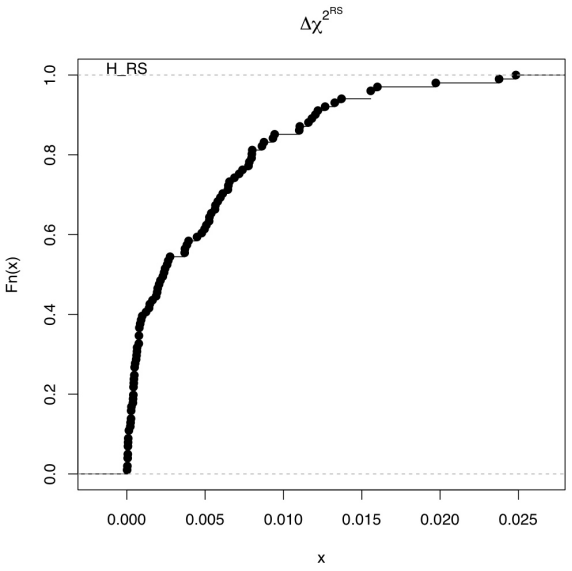

Fig. 9: Cumulative histogram of $\Delta\chi^2$ obtained for the 101 resampled runs.

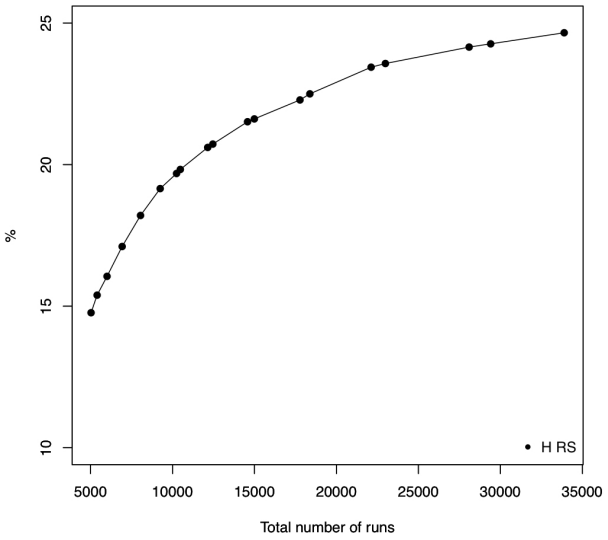

Fig. 10: Evolution of the number of selected ephemerides based on the resampling criteria described in the text.

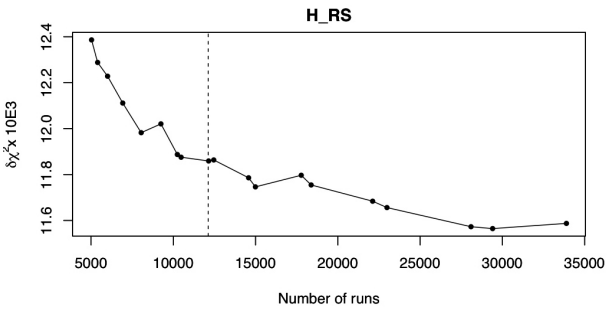

Fig. 11: Evolution of the average values of $\delta\chi^2$ (y-axis) regarding the total number of ephemerides (x-axis) selected with the resampling criteria.

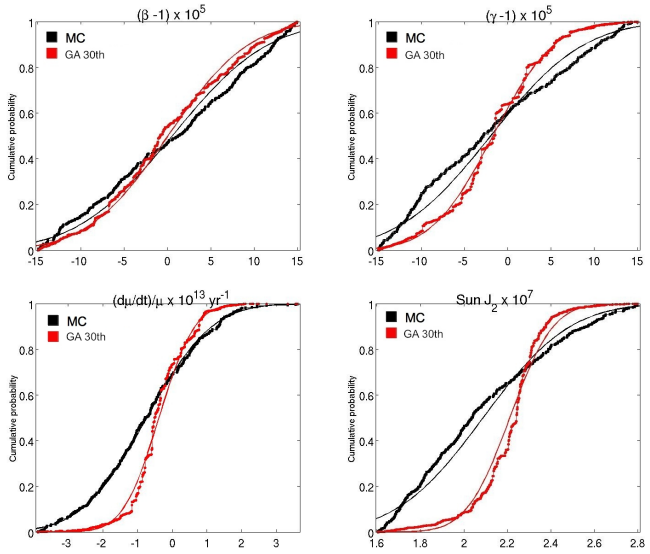

Fig. 12: Cumulative histogram of (PPN β, PPN γ, $J_2^\odot$, $\dot{\mu}/\mu$) for the generation 0 of ephemerides selected with the resampling criteria (noted MC and colored in black) and for the final generation noted GA 30^{th} and colored in red also selected with the resampling criteria. The full lines are the corresponding cumulative histograms for the normal distribution fitted on the distributions of the first generation and the 30th generation.

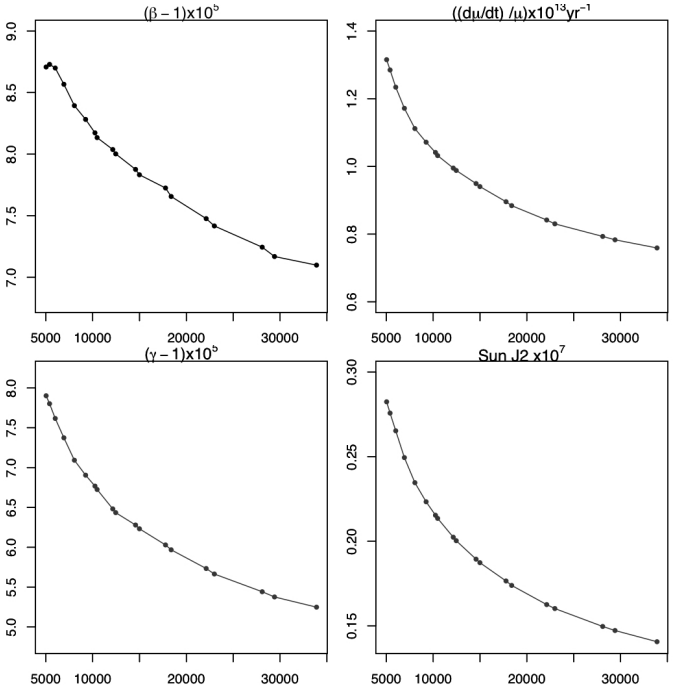

Fig. 13: Evolution with the number of selected runs of the 1-σ of the gaussian distribution of the PPN β, PPN γ, $J_2^\odot$, and $\dot{\mu}/\mu$ parameters corresponding to the ephemerides selected with the resampling criteria.

6. Discussions

On Table 2 are gathered the results obtained with this work as well as very diverse estimations found in the literature. If one wants to exhibit one single set of values of acceptable intervals for the four parameters randomly modified in this work, one can consider the mean values of the most numerous selection presented in Table 2, gathering values of (PPN β, PPN γ, $J_2^\odot$, $\dot{\mu}/\mu$) inducing ephemerides with $\Delta(O-C)_{max} < 50\%$ and ephemerides selected with the resampling criteria. By considering the mean of these two selections, we then obtain the values labeled MC + GA (50 % + RS) in Table 2.

As noticed in Verma et al. (2014) the interval of possible violations for the PPN parameters β and γ with no time variation of the Newtonian gravitational constant G and in fixing the value of the Sun flattening is as accurate as the reference values obtained with the Cassini experiment (Bertotti et al. (2003)).

However by adding the variations of $\dot{\mu}/\mu$ and $J_2^\odot$, we have enlarge the possible interval of violations for the four parameters as given in line MC + GA (50 % + RS) of Table 2. This result is consistent with the fact that these parameters are linked through their influences on the orbital elements of the planets as described by Equation 1. In opposition to Pitjeva & Pitjev (2013), β intervals are always larger than γ intervals. This can be explained again by the Equation 1. The determination of PPN β can only be done with this equation where $\dot{\mu}/\mu$ and $J_2^\odot$ influences can mix up with those of β and γ. In the meantime, PPN γ can be constrained by the Shapiro delay where only $\dot{\mu}/\mu$ plays a role with γ. The β intervals deduced from LLR analysis are still larger than those obtained in this work. The LLR determinations are based only on the modeling of the Moon

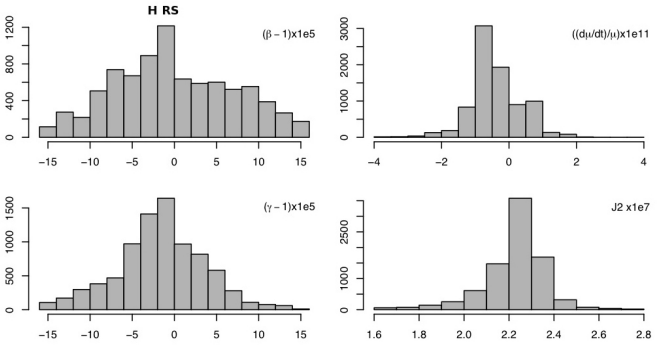

Fig. 14: Histograms of the distribution of the PPN β, PPN γ, $J_2^\odot$, and $\dot{\mu}/\mu$ parameters corresponding to the ephemerides selected with the resampling criteria for the full sample of simulated ephemerides.

orbit about the Earth. As explained in introduction, the planetary ephemerides provide better determinations of PPN parameters thanks to the eight equations of motion considered in the computations. The acceptable interval of $\dot{\mu}/\mu$ deduced from this work is surprisingly a factor 2 more narrow than the one deduced from LLR analysis. This can again be explained by the disentangling operated between the gravitational signatures of PPN β, PPN γ, $J_2^\odot$, $\dot{\mu}/\mu$ by considering the eight planetary equations of motion simultaneously. Comparisons to Pitjeva & Pitjev (2013) seem to be difficult as no clear evidence of a simultaneous fit of the four considered parameters is given in their paper. In the other hand, as Pitjeva & Pitjev (2013) values are directly extracted from a least square procedure, we

can expect to have small uncertainties from the least square determinations in comparison to our statistic intervals of violation including all correlations. Values extracted from Konopliv et al. (2011) were obtained with planetary ephemerides built before the use of Messenger tracking data in their construction. The subsequent improvement of the Mercury orbit is then not included in Konopliv et al. (2011) results but in Folkner et al. (2014) and its value of $J_2^{\odot}$. Future JPL estimations of PPN parameters and $\dot{\mu}/\mu$ should also benefit from the improved Mercury orbit.

Finally, values obtained by astrophysical technics such as heliosismology or pulsar timing analysis are less restrictive than those obtained in the solar system. However, considering all the given figures of Table 2 one should conclude that no deviation to general relativity is noticeable for the four parameters modified simultaneously.

7. Conclusions

In this work we have estimated new limits of possible violations of general relativity with the PPN parameters β, γ in considering in the same time time variations of the Gravitational constant G and various values of the sun flattening. We used Monte Carlo simulations and genetic algorithm procedures for producing more than 35000 planetary ephemerides fitted to observations and compared to INPOP13c. Different criteria have been used for characterizing the closest ephemerides from INPOP13c and so, for identifying the most acceptable intervals of parameters inducing the smallest modifications to the planetary dynamics.

New tests will be implemented such as the addition of supplementary terms in the equation of motions of the planets as proposed by alternative theories (Blanchet & Novak (2011), Hees et al. (2014), Jaekel & Reynaud (2011)). Tests of the equivalence principal can also be proposed for Monte Carlo simulations and genetic algorithm procedures. In the case of the planetary orbits, one would have to consider one ratio of gravitational and inertial masses for each planet which would multiply the number of runs by an important scale.

Acknowledgments

This work benefited from HPC resources of MesoPSL financed by the Region Ile de France and the project Equip@Meso (reference ANR-10-EQPX-29-01) of the programme Investissements d'Avenir supervised by the Agence Nationale pour la Recherche. The authors thank also Professor Damour for his fruitfull discussions.

References

Bambi, C., Giannotti, M., & Villante, F. L. 2005, Phys. Rev. D, 71, 123524
Beaugé, C., Ferraz-Mello, S., & Michtchenko, T. A. 2012, Research in Astronomy and Astrophysics, 12, 1044
Bertotti, B., Iess, L., & Tortora, P. 2003, Nature, 425, 374
Blanchet, L. & Novak, J. 2011, MNRAS, 412, 2530
Busing, F.-M., Meijer, E., & Van der Leeden, R. 1999, Statistics and Computing, 9, 3
Charbonneau, P. 1995, ApJS, 101, 309
Cook, R. D. & Weisberg, S. 1982, Residuals and Influence on regression (New York, USA: Champman and Hall)
Damour, T., Gibbons, G. W., & Gundlach, C. 1990, Physical Review Letters, 64, 123
Damour, T. & Nordtvedt, K. 1993, Phys. Rev. D, 48, 3436
Damour, T. & Polyakov, A. M. 1994, General Relativity and Gravitation, 26, 1171
Einstein, A. 1913, in The Genesis of General Relativity, ed. J. Renn, M. Janssen, J. D. Norton, T. Sauer, J. Stachel, L. Divarci, M. Schemmel, C. Smeenk, & C. Martin, 543
Fay, R. E. 1985, Journal of the American Statistical Association, 80, 148
Fienga, A., Laskar, J., Kuchynka, P., et al. 2010, American Astronomical Society, IAU Symposium #261. Relativity in Fundamental Astronomy: Dynamics, Reference Frames, and Data Analysis 27 April - 1 May 2009 Virginia Beach, VA, USA, #6.02; Bulletin of the American Astronomical Society, Vol. 41, p.881, 261, 602
Fienga, A., Laskar, J., Manche, H., Gastineau, M., & Verma, A. 2014, New INPOP release: INPOP13c, ArXiv e-prints
Fienga, A., Laskar, J., Manche, H., et al. 2011, Celestial Mechanics and Dynamical Astronomy, 111, 363
Fienga, A., Laskar, J., Morley, T., et al. 2009, A&A, 507, 1675
Folkner, W. M., Williams, J. G., Boggs, D. H., Park, R. S., & Kuchynka, P. 2014, Interplanetary Network Progress Report, 196, C1
Francis, M. P. 1965, AJ, 70, 675
Füzfa, A. & Alimi, J.-M. 2007, Phys. Rev. D, 75, 123007
Goździewski, K., Nasiroglu, I., Słowikowska, A., et al. 2012, MNRAS, 425, 930
Guenther, D. B., Krauss, L. M., & Demarque, P. 1998, Astrophys. J., 498, 871
Hees, A., Folkner, W. M., Jacobson, R. A., & Park, R. S. 2014, Phys. Rev. D, 89, 102002
Hees, A., Lamine, B., Reynaud, S., et al. 2012, Classical and Quantum Gravity, 29, 235027
Henke, S., Gail, H.-P., Trieloff, M., & Schwarz, W. H. 2013, Icarus, 226, 212
Hofmann, F., Müller, J., & Biskupek, L. 2010, A&A, 522, L5
Horner, J., Wittenmyer, R. A., Hinse, T. C., & Tinney, C. G. 2012, MNRAS, 425, 749
Jaekel, M.-T. & Reynaud, S. 2011, Mass, Inertia, and Gravitation, ed. L. Blanchet, A. Spallicci, & B. Whiting, 491–530
Karnath, N., Prato, L., Wasserman, L. H., et al. 2013, AJ, 146, 149
Kaspi, V. M., Taylor, J. H., & Ryba, M. F. 1994, Astrophys. J., 428, 713
Konopliv, A. S., Asmar, S. W., Folkner, W. M., et al. 2011, Icarus, 211, 401
Lambert, S. B. & Le Poncin-Lafitte, C. 2009, A&A, 499, 331
Le Verrier, U. J. 1859, Annales de l'Observatoire de Paris, 5, 1
Li, Y.-C., Wu, F.-Q., & Chen, X. 2013, Phys. Rev. D, 88, 084053

Luzum, B., Capitaine, N., Fienga, A., et al. 2011, Celestial Mechanics and Dynamical Astronomy, 110, 293
Magnin, V. 1998, PhD in electronics, University Lille 1
Marty, J.-C. 2013, Mars Odyssey data release, private communication
Migaszewski, C., Słonina, M., & Goździewski, K. 2012, MNRAS, 427, 770
Morley, T. 2012, MEX and VEX data release, private communication
Morley, T. 2013, MEX and VEX data release, private communication
Moyer, T. 2000, Formulation for Observed and Computed Values of Deep Space Network Data Types for Navigation, Monography of DEEP SPACE COMMUNICATIONS AND NAVIGATION SERIES 2, JPL
Müller, J., Soffel, M., & Klioner, S. A. 2008, Journal of Geodesy, 82, 133
Nowak, G., Niedzielski, A., Wolszczan, A., Adamów, M., & Maciejewski, G. 2013, ApJ, 770, 53
Pinto, R. F., Brun, A. S., Jouve, L., & Grappin, R. 2011, ApJ, 737, 72
Pitjeva, E. V. & Pitjev, N. P. 2013, MNRAS, 432, 3431
Siqueira Mello, C., Hill, V., Barbuy, B., et al. 2014, A&A, 565, A93
Steinhardt, P. J. & Wesley, D. 2009, Phys. Rev. D, 79, 104026
Uzan, J.-P. 2003, Annales Henri Poincaré, 4, 347
Verma, A. K. 2013, PhD in astronomy, Université de Besancon, France.
Verma, A. K., Fienga, A., Laskar, J., Manche, H., & Gastineau, M. 2014, A&A, 561, A115
Williams, J. G. & Folkner, W. M. 2009, in IAU Symposium #261, American Astronomical Society, Vol. 261, 801
Williams, J. G., Turyshev, S. G., & Boggs, D. H. 2004, Physical Review Letters, 93, 261101
Williams, J. G., Turyshev, S. G., & Boggs, D. H. 2009, International Journal of Modern Physics D, 18, 1129

Appendix A: INPOP13c data sample and postfit residuals

Table A.1: Statistics (means and 1-σ standard deviations) of the residuals obtained after the INPOP13c fit for common data sample between INPOP13c and INPOP10e.

Type of data		Nbr	Time Interval	INPOP10e		INPOP13c	
Mercury	range [m]	462	1971.29 - 1997.60	-45.3	872.5	-101.5	861.5
Mercury Mariner	range [m]	2	1974.24 - 1976.22	-31.8	109.2	-196.4	19.6
Mercury flybys Mess	ra [mas]	3	2008.03 - 2009.74	0.7	1.5	0.9	1.3
Mercury flybys Mess	de [mas]	3	2008.03 - 2009.74	2.4	2.5	2.5	2.4
Mercury flybys Mess	range [m]	3	2008.03 - 2009.74	-5.1	5.8	3.2	7.7
Venus	VLBI [mas]	46	1990.70 - 2010.86	1.6	2.6	1.6	2.6
Venus	range [m]	489	1965.96 - 1990.07	500.2	2234.9	504.6	2237.6
Venus Vex	range [m]	22145	2006.32 - 2009.78	-0.0	4.1	1.0	5.1
Mars	VLBI [mas]	96	1989.13 - 2007.97	-0.0	0.4	0.0	0.4
Mars Mex	range [m]	13842	2005.17 - 2009.78	0.4	3.2	-0.5	1.8
Mars MGS	range [m]	13091	1999.31 - 2006.83	-0.3	3.8	0.4	3.8
Mars Ody	range [m]	5664	2006.95 - 2010.00	0.3	4.1	1.5	2.3
Mars Path	range [m]	90	1997.51 - 1997.73	-6.3	13.7	19.3	14.1
Mars Vkg	range [m]	1257	1976.55 - 1982.87	-1.4	39.7	-1.5	41.2
Jupiter	VLBI [mas]	24	1996.54 - 1997.94	-0.3	11.068	-0.450	11.069
Jupiter	ra [mas]	6532	1914.54 - 2008.49	-39.0	297.0	-39.0	297.0
Jupiter	de [mas]	6394	1914.54 - 2008.49	-48.0	301.0	-48.0	301.0
Jupiter flybys	ra [mas]	5	1974.92 - 2001.00	2.4	3.2	2.5	3.0
Jupiter flybys	de [mas]	5	1974.92 - 2001.00	-10.8	11.5	-10.8	11.4
Jupiter flybys	range [m]	5	1974.92 - 2001.00	-907.0	1646.2	-986.0	1775.6
Saturne	ra [mas]	7971	1913.87 - 2008.34	-6.0	293.0	-6.0	293.0
Saturne	de [mas]	7945	1913.87 - 2008.34	-12.0	266.0	-12.0	266.0
Saturne VLBI Cass	ra [mas]	10	2004.69 - 2009.31	0.215	0.637	0.113	0.630
Saturne VLBI Cass	de [mas]	10	2004.69 - 2009.31	0.280	0.331	-0.115	0.331
Saturne Cassini	ra [mas]	31	2004.50 - 2007.00	0.790	3.879	0.663	3.883
Saturne Cassini	de [mas]	31	2004.50 - 2007.00	6.472	7.258	5.906	7.284
Saturne Cassini	range [m]	31	2004.50 - 2007.00	-0.013	18.844	0.082	23.763
Uranus	ra [mas]	13016	1914.52 - 2011.74	7.0	205.0	7.0	205.0
Uranus	de [mas]	13008	1914.52 - 2011.74	-6.0	234.0	-6.0	234.0
Uranus flybys	ra [mas]	1	1986.07 - 1986.07	-21.0	0.000	-21.0	0.000
Uranus flybys	de [mas]	1	1986.07 - 1986.07	-28.0	0.000	-28.0	0.000
Uranus flybys	range [m]	1	1986.07 - 1986.07	19.7	0.000	20.8	0.000
Neptune	ra [mas]	5395	1913.99 - 2007.88	0.0	258.0	3.0	258.0
Neptune	de [mas]	5375	1913.99 - 2007.88	-0.0	299.0	-2.0	299.0
Neptune flybys	ra [mas]	1	1989.65 - 1989.65	-12.0	0.000	-11.0	0.000
Neptune flybys	de [mas]	1	1989.65 - 1989.65	-5.0	0.000	-5.0	0.000
Neptune flybys	range [m]	1	1989.65 - 1989.65	69.6	0.000	51.5	0.000
Pluto	ra [mas]	2458	1914.06 - 2008.49	34.0	654.0	20.0	574.0
Pluto	de [mas]	2462	1914.06 - 2008.49	7.0	539.0	1.0	525.0
Pluto Occ	ra [mas]	13	2005.44 - 2009.64	3.0	47.0	-100.0	44.0
Pluto Occ	de [mas]	13	2005.44 - 2009.64	-6.0	18.0	0.0	27.0
Pluto HST	ra [mas]	5	1998.19 - 1998.20	-33.0	43.0	-18.0	44.0
Pluto HST	de [mas]	5	1998.19 - 1998.20	28.0	48.0	-26.0	48.0

Table A.2: Statistics of INPOP13c postfit residuals for new samples included in the fit. For comparison, means and standard deviations of residuals obtained with INPOP10e on these prolongated intervals are also given.

Type of data		Nbr	Time Interval	INPOP10e		INPOP13c	
Mercure Messenger	range [m]	371	2011.39 - 2013.20	7.2	189.7	4.0	12.4
Venus Vex	range [m]	2825	2009.78 - 2011.45	1.8	16.5	5.1	15.7
Mars Mex	range [m]	12268	2009.78 - 2013.00	3.6	23.3	1.2	5.6
Mars Ody	range [m]	3510	2010.00 - 2012.00	4.8	9.6	0.7	1.8